Hindawi
Shock and Vibration
Volume 2022, Article ID 8303722, 11 pages
https://doi.org/10.1155/2022/8303722

Research Article

A Novel Denoise Method of Acoustic Signal from Train Bearings Based on Resampling Technique and Improved Crazy Climber Algorithm

Yali Sun,[1] **Hua Li**,[2] **Xing Zhao**,[2] **Jiyou Fei**,[2] **Xiaodong Liu**,[2] **and Yijie Niu**[3]

[1]*College of Mechanical Engineering, Dalian Jiaotong University, Dalian 116028, China*
[2]*College of Locomotive and Rolling, Dalian Jiaotong University, Dalian 116028, China*
[3]*College of Software, Dalian Jiaotong University, Dalian 116028, China*

Correspondence should be addressed to Jiyou Fei; fjy@djtu.edu.cn

Received 29 November 2021; Accepted 2 March 2022; Published 24 March 2022

Academic Editor: Kexiang Wei

The wayside acoustic defective bearing detector system (TADS) is located on both sides of the railway, so that the acoustic signals recorded by the microphone not only include the sound from the train bearings but also include it from the other disturbance sources. The heavy noise and multisource acoustic signals would badly reduce the reliability and accuracy of the detection result of the TADS. In order to extract the useful information from the recorded signal exactly and efficiently, a novel denoising method based on the Short-time Fourier transform (STFT) and improved Crazy Climber algorithm was improved in this paper. Firstly, the STFT was performed on the recorded acoustic signals in order to obtain the time-frequency distribution matrix. Based on the original algorithm, the novel movement rule and the fitting process of the ridge lines were presented which could extract the time-frequency ridge lines of the acoustic signal accurately and rapidly. In this way, the important information from the train bearings could be divided from the heavy noise and other signals. Finally, the simulation and experimental verifications were carried out, and the denoising method based on the STFT and improved Crazy Climber algorithm has proved to be effective in extracting ridge lines of the time-frequency distribution matrix and dividing the useful information form the recorded acoustic signals.

1. Introduction

The failure of the rolling bearings has already become one for the main reasons of the train breakdown in the past decade, which could lead to irretrievable loss of life and property in serious cases. Therefore, it is essential to develop the techniques of fault diagnosis and condition monitoring for the train bearings in the transportation industry [1–4]. The wayside acoustic defective bearing detector system (TADS) [5] was developed in the 1980s to detect bearing flaws, which could collect the acoustic signal from the bearings of trains by monitoring microphones on the rail-mounted wayside [6–8]. And, the service status monitoring of the train bearings can be realized by processing and analyzing the acoustic signals. Just one set of such systems could be used to monitor all the trains passing through the section, which improves the efficiency of bearing monitoring and reduces the monitoring cost greatly [9–11]. Meanwhile, the TADS has some unique characteristics as no-contact and no-disintegration versus traditional contact measurement (vibration-based methods). Therefore, the wayside acoustics-based techniques have aroused considerable interest over the past years in the field of train monitoring. However, some key issues still need to be solved, such as there is serious noise in received acoustic signals. Besides the important information from the train bearing, the audio signals usually contain lots of useless content like the ambient noise, the rolling noise, the air-noise and traction noise. What is important is that the intensity of the noise signal in the received signal is much greater than that of the bearing signal, and the signals from various sources are mixed together, which makes it difficult to obtain useful signals effectively, so that it is still a great

challenge for train bearing detecting with acoustic methods at present.

There are some scholars being committed to the problem mentioned above. Yu-xing and Long [12] proposed a novel noise reduction method for underwater acoustic signals. Such method was based on the complete ensemble empirical mode decomposition with adaptive noise, minimum mean square variance criterion and least mean square adaptive filter. This method has a better performance on suppression of mode mixing and also has a better noise reduction performance. Moreover, it is beneficial to the further processing of underwater acoustic signals. Ni et al. [13] proposed a fault information-guided variational mode decomposition method for extracting the weak bearing information. In this method, the sensitivity to the bearing fault signature, which was achieved through the integration of the bearing fault cyclic period, enables early bearing fault diagnosis competently. The method mentioned above provided a good reference for noise reduction and bearing fault diagnosis. However, due to the special position of TADS, the signals received by the microphone are not repeatable, so it is still difficult to effectively detect train bearings. And other scholar found that the ridge energy intensity of the bearing's time domain signal was much higher than that of the noise and other useless signals. In addition, the instantaneous frequency (IF) of the bearing signal can be obtained by the ridges of the time-domain signal, and the objects of denoise and bearings diagnosis could be achieved. Zhang et al. [14]. proposed a time-frequency ridge extract method based on instantaneous frequency estimation. By this method, the ridge lines of the signal could be extracted completely in the case of low noise. To some extent, this method realized the noise cancellation and useful signals extraction. Xu et al. [15] aiming at the problem of the ridge lines could not extract completely, they propose to extract the instantaneous the ridge lines of sound signal effectively by compressing and rearranging the time spectrum in the time-frequency plane under the low noise environment. The method mentioned above provides good references and experience for extracting time-frequency ridge lines. However, these denoising methods based solely on frequency domain processing have poor performance in high ambient noise and can only extract useful information in low noise environment. However, there is a lot of noise in the sound signal received by the microphone, which limits the application of the above method in practical application.

Further, some researchers are looking for ways to remove noise and extract useful information in higher-noise environments. The Crazy Climber algorithm was proposed by Carmona et al. [16], which could extract multiple instantaneous frequencies at the same time under a certain degree of strong noise interference. Such algorithm has been demonstrated valid in extracting the ridges of the signal with multi-ridges in higher-noise environments, which makes it convenient to obtain the IFs based on the time-frequency domain. So the Crazy Climber algorithm has already attracted the attention of research institutions and detector system equipment manufacturers at present.

Some scholars extracted the ridge lines of the time-frequency domain with this algorithm directly in their own research. Such as Kailiang Xu et al. [17] and Li et al. [18], in their research, the wavelet transform method is used to obtain the time-frequency matrix, and the ridge lines of the time-frequency matrix is obtained through the Crazy Climber algorithm, and finally the acoustic detection of train bearings is realized. Chen and Xu [19] proposed a method similar to Li et al. [18]. Unlike the research mentioned above, they obtained the frequent-domain signal by the Fourier transform. In addition to this, some similar strides have been done by some other researchers [8, 20–23]. Their research has achieved noise reduction in high noise environment to a certain extent and extracted useful train bearing signals, but there are still some problems such as incomplete extraction of ridge lines and inconsistency between the instantaneous frequency obtained and the actual frequency. And some scholars consider such issues were caused by the low accuracy of the frequent-domain signal. Therefore, they further improve the extraction method of time-frequency matrix. Zheng et al. [24] proposed a method to improve the accuracy of time-frequency matrix though the continuous wavelet transform. After this, the Crazy Climber algorithm was used to extract the ridge lines from the high-precision frequent-domain signal. Hu et al. [25] and Wang et al. [26] came up with a similar approach that was used to extract the ridge lines. What's different is that they improved the accuracy of the frequent-domain signal with the method of the short-time Fourier transform (STFT). Although the accuracy of time-frequency matrix is quite improved effectively, it is still difficult to identify the whole ridge lines when extracting it with Crazy Climber algorithm. As a result, there is still a deviation between the extracted ridge line and the actual ridge line. Meanwhile, the effect of noise removal is not obvious, and it is difficult to accurately extract useful information. Therefore, some scholars recognize that may the Crazy Climber algorithm exist defects which lead to it being deficient in ridge lines recognition among higher noise. So they try to improve the ridge extract ability of the algorithm itself. For example, Lin and Zhang [27] and Peng et al. [28] attempted to make changes to the metric matrix of the Crazy Climber algorithm. They changed the counting function of the metric matrix and the move frequency of the climbers, which improved the speed of the algorithm greatly, but had little effect on the accuracy.

In summary, the Crazy Climber algorithm still has some disadvantage at present. The particles have disordered phenomena in the process of moving and unable to effectively avoid the low energy points, which will be resulting in particles cannot be accurately reach high frequency energy region. In addition, because the starting point is randomly selected during the extraction of ridge line, it takes a long time to extract ridge line, and it also causes the extracted ridge line to be not smooth, and even some high energy points are omitted. These problems lead to the low recognition accuracy of ridge line extraction in high noise environment. And simultaneous extraction of multiple signals requires a variety of complex processing, resulting in incomplete and inefficient extraction of ridges.

Aiming at the difficulties and present situation of noise reduction in acoustic diagnosis of train bearing defects with multi-source separation, a denoising method based on short-time Fourier transform (STFT) and an improved Crazy Climber algorithm is proposed. Firstly, the short-time Fourier transform is used to extract the time-frequency matrix from the received acoustic signal. Then, the crazy climber algorithm is improved. By changing the motion law of the particles (climbers) in the metric matrix, it can actively avoid the low energy point it has passed under any circumstances, and then can reach the high energy point more accurately and faster. The extraction rule of local optimal peak value was changed. The center time of time-frequency matrix is taken as the starting point of ridge line extraction and the location of local optimal peak value is determined by multiple points. This can make the extracted ridge line more smooth and accurate. Finally, the performance of the method is verified by simulation and experiment. The results show that this method can extract ridge effectively and accurately in high noise environment.

2. The Crazy Climber Algorithm and Improve Method

2.1. The Crazy Climber Algorithm. The Crazy Climber algorithm is a ridge lines extraction method based on Markov chain. The main idea of this algorithm is as follows: Firstly, a large number of points are scattered in the time-frequency randomly, and each of them could be regarded as the density distribution. Then each particle moves in the region according to the transition mechanism of the Markov chain. And they are gradually attracted to the position of ridges which distribution on the plane of the time-frequency. The rule of the motion on the horizontal axis is the standard symmetric random walk, and it on the vertical axis is like climbing a mountain, so that, these randomly distributed points also could be called climbers. The processing of climbers reaching the ridges is also like the simulated annealing algorithm, and according to this algorithm, all the ridges of the time-frequency curve could be finally found. The system needs to set an initial temperature *Ttemp*, and as the temperature drops, the particles that can move stabilize and eventually converge into the high energy area where the ridge is located.

The processing of this algorithm as shown in Figure 1, and it could be divided into two parts, the one is the movement process of the Climbers and the other one is looking for the appropriate ridge lines. There are four steps in the first part and three steps in the second part. Assume the discussed time-frequency domain is $\mathbf{T}(j, k)$ which size is $B \times A$, and it represents the value at position (j, k) in time-frequency distribution. In the horizontal axis $j = 1, 2, \ldots, B$, and in the vertical axis $k = 1, 2, \ldots, A$.

The operational process of the Crazy climber algorithm is described as follows, and each climber is independent of each other. Create and initialize the metric matrix **D**, the Times of move n, and the number of the climbers N, And the N is determined by the size of the domain **T**. The climbers

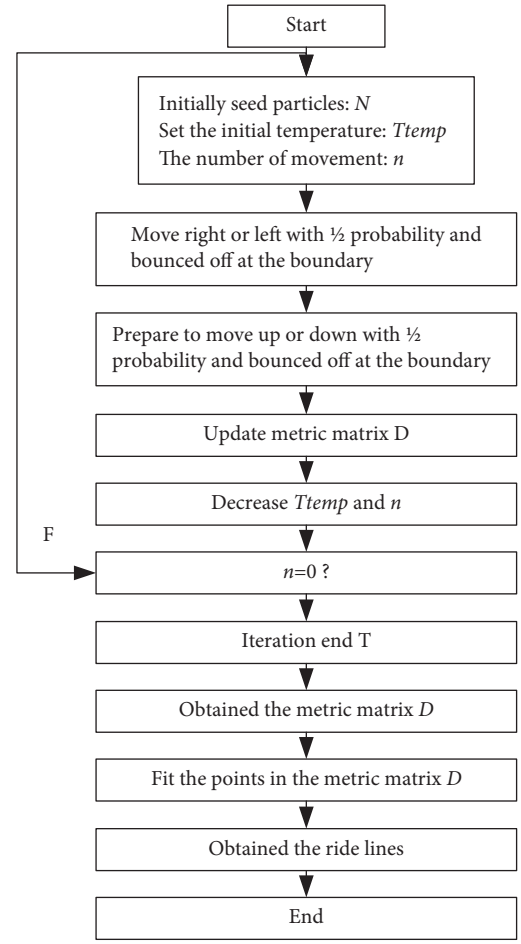

Figure 1: Flowchart of the Crazy Climber algorithm.

are evenly distributed on grid **S**, which could described as follow: $\mathbf{S} = \{1, 2, \ldots, B\} \times \{1, 2, \ldots, A\}$

The maximum number of Climbers N will not be more than $B \times A$. The initial position of the particle is $X_a(0)$, and $a = 1, 2, 3, \ldots, N$.

(1) After setting the necessary parameters, assuming that the initial temperature of the system is Ttemp, and a particle stays at the position $X_a(t) = (j, k)$ at some time t, then its next position (j', k') will be determined by two conditions. Firstly, the particle moves horizontally. If j is between 2 and $B - 1$, then $j' = j - 1$ or $j' = j + 1$ both of which have the same probability of 50%. If the particle is exactly on the boundary, then it will move one space in the opposite direction, that is, if $j = 1$, then $j' = j + 1$, and if $j = B$, then $j' = j - 1$. After horizontal movement, the particle moves vertically. The movement rule in the vertical direction is similar to that in the horizontal direction, with a 50% probability of moving up or down (the same rule at the boundary as in the horizontal direction), but it is also possible to make no movement, but if the particle must move, i.e. $X_a(t + 1) = (j', k')$. The probability of particle movement is p_k. p_k can be expressed by the following formula.

$$p_k = \exp\left\{\frac{[T(j',k') - T(j',k)]}{T_k}\right\}, \quad (1)$$

where $T_k = [\max(T) - \min(T)]/\log_2^k$.

In this case, the probability of not moving is $1 - p_k$. And after the move, the temperature of the system is update to $T_{\text{temp}+1}$. When the temperature of the system falls below a certain threshold, the iterative moving process ends.

(2) After the iteration has been completed, each point on the metric matrix D needs to be measured. At time t, a particle moves to a certain position $X_a(t)$, and the point corresponding to this position in the metric matrix **D** needs to be added by 1. Assuming that each Climber corresponds to a mass of $1/N$, it can be considered that the metric of the metric matrix and the metric of the final metric matrix at time t are

$$D(t) = \frac{1}{N} \cdot \sum_{a=1}^{N} \delta(X_a(t) - S). \quad (2)$$

In order to further improve the accuracy of extracted ridge line and make the change of ridge line parameters more close to the change of parameters on the original time-frequency plane, it is necessary to weight the measurement values, so the weighted measurement value is

$$D_e(t) = \sum_{a=1}^{N} E \cdot \delta(X_a(t) - S). \quad (3)$$

Meanwhile, since the movement of each moving point is a random process, the measurement value is also a random quantity. Therefore, in order to make the final measurement to each grid point, the mean value of the measurement value is needed to represent the measurement value. And, the mean value of the measurement value is expressed as

$$D^I = \frac{1}{T_{\text{time}}} \sum_{t=1}^{T_{\text{time}}} D(t),$$
$$D_e^I = \frac{1}{T_{\text{time}}} \sum_{t=1}^{T_{\text{time}}} D_e(t), \quad (4)$$

where T_{time} is the total length of time.

After all the ridge lines are obtained, the length of each ridge line is calculated and the length threshold value is determined. The ridge lines which are shorter than threshold value will be eliminated and the remaining ones will be extracted.

What should be noticed is that take into account the effect of noise a threshold value e should be decided before step 5 in order to pull the ridge lines out from low measurement value in Dn. And the threshold should be set as the integral multiple of the mean value or the decimal multiple of the maximum value of the metric matrix. This process could be written as the following equation:

$$D_n(i,j) = \begin{cases} D_n(i,j) & D_n(i,j) \geq e \\ 0 & D_n(i,j) < e \end{cases}. \quad (5)$$

After the process mentioned above, the ridge points are clearly visible. Since the instantaneous frequency is a curve slowly changing along the time axis. So, the algorithm will start at the left end of the grid and extract the ridge point along the time axis that is close to the frequency coordinate of the ridge point at the previous point as the ridge point frequency value at the next point. And connect the two points to form a ridge line and repeat the process until all ridge lines are found.

2.2. Evolutionary Rules. As described about the Crazy Climber algorithm in Section 2.1, it could be found that although such an algorithm could extract multiple ridge lines at the same time, what should be noticed is that, the processing speed of the algorithm depends on the number of the climbers. When the magnitude of climbers is very huge, it will take up so much time to compute. But on the contrary, the accuracy of the algorithm will be declining. Therefore, it is very important to improve the accuracy under the condition of finite particles. It is necessary to improve the rules of particle movement and ridge extraction. In the traditional Crazy Climbing algorithm, the movement of particles is random, and it takes several iterations to make the particles reach the high energy position, or even repeatedly reach the position that the particles have already passed through, which leads to the low efficiency of obtaining the metric matrix. At the same time, the process of fitting the ridge after obtaining the ridge point is also accompanied by randomness. The ridge starts fitting from the zero point of the time axis. In this process, it is difficult to find the maximum value and effective value of the metric matrix quickly and accurately, so the extracted ridge is not necessarily the real matrix of the system.

Aim such problems, an improved crazy climber algorithm was put forward in this part. The rules of particles movement and the fitting process of ridge lines are improved based on the original algorithm. The basic implementation process is as follows:

(1) In order to improve the accuracy and efficiency of the metric matrix, a novel movement rule of the climbers in time-frequency domain is proposed which makes it could move towards the ridge lines faster. Assume that the position corresponding to particle at tk is $X_a(t_k) = (j,k)$, then the position corresponding to the particle at $tk+1$ is $X_a(t_{k+1}) = (j',k)$, and at $tk+2$ is $X_a(t_{k+2}) = (j',k')$.

As shown in Figure 2, each block represents where the particle is likely to move in. It is assumed that the particle is at A5 (j,k) at $t = tk$, According to the movement rule of the algorithm, the particle will move left and right at $t = tk+1$ (A2 and A8, (j',k)). And the probability of movement at this time will be affected by the corresponding frequency amplitude of the particle at $t = tk$ and $t = tk+1$. Zu is assumed to be the increment between the amplitude of two

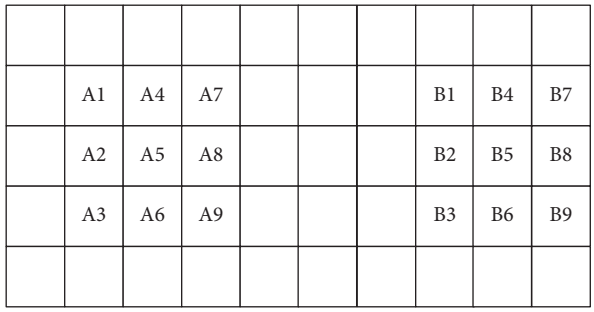

Figure 2: Schematic diagram of Climber movement.

positions, and the larger the increment is, the greater the probability of moving to the position of this point is. The movement probability is calculated by the following formula:

$$P_z = \frac{Z_u}{\sum_1^2 \left(Z_u + \left|\min\left(S\left(X_a\left(t_k\right)\right)\right) - S\left(\left(X_a\left(t_{k+1}\right)\right)\right)\right|\right)},$$
$$Z_u = \left(S\left(X_a\left(t_k\right)\right)\right) - S\left(\left(X_a\left(t_{k+1}\right)\right)\right). \quad (6)$$

Assuming the particle move to A8 at $t = tk + 1$. In the following movement, the traditional algorithm is used to determine whether the particle moves or does not move. If it moves, then at $t = tk + 2$, the particle moves toward A7 or A9 according to the above probability. If it does not move, at $t = tk + 3$, the particle is still at A8, and at $t = tk + 4$, the particle starts to move left and right. Since A5 is the point that the particle has passed, the probability of moving to A5 is 0, and the probability of moving to the right is 100%.

The rules for particle movement at the boundary are slightly different. It can be explained as follows: assume the particle at the location B5 at $t = tk$ as shown in Figure 1, it could only in block B2 or B8 in the next movement. It will follow the rules of movement above if the particle in the block B2. Assume that the particle in the block B8 at $t = tk + 1$. If it moves, then the particle may appear at B7 or B9, and at the next moment, the iteration starts again. If it does not move, If the particle does not move, the frequency increment of B4~B9 relative to B8 should be calculated and the probability of movement also should be recalculated. According to the new movement rules, particles can effectively avoid passing through a point repeatedly, and can quickly reach the high energy region. In this way, the efficiency and accuracy of extracting the ridge lines could be improved sharply.

(2) On the condition of actual working, there is not only noise or multi-source signal in the acoustic signal received by microphone but also be influenced by the Doppler effect, which results in distorting. It is worth noting that, after eliminating the distortion through STFT, it can be found the situation of distortion at the center time of signal (the straight-line distance between the train and the microphone is the shortest) is the minimum. That is, the difference between the received signal and the actual signal generated by the bearing is the minimum at that time. Therefore, it can be judged that the ridge lines through the center time in the time-frequency matrix must belong to the useful signals. So that, taking the center time as the starting position can be more accurate and rapid than taking random point as the starting position for fitting the ridge lines. In addition, the process of fitting ridge lines will also be improved.

The selection fitting point at a certain time will be affected by the points at the previous two times. For example, the fitting point is C1 at tk, and C2 at $tk + 1$, then the direction of the selected fitting point at time t is the connecting line direction of C1 and C2. If the connecting line direction is pointing the C3 at time $tk + 2$, and the C4 and C5 are the nearest points to C3 in the vertical direction. Then the fitting point at time t should be the peak value among C3, C4 and C5, as shown in Figure 3. It can be found that the smoothness and accuracy of the ridge lines can be improved by the improved fitting method mentioned above.

3. Simulation Signal Analysis

3.1. Simulation Signal Construction. Effects of the improved denoise method on extracting ridge lines were verified by simulation and experimental. An acoustic signal with Gaussian white noise is built as follows:

$$\begin{cases} \mathrm{sig}_1(t) = 0.5\ \sin\left(40\ \sin\left(4\pi t\right) + 1600\pi t\right), \\ \mathrm{sig}_2(t) = 0.5\ \cos\left(700\pi t\right), \\ \mathrm{sig} = \mathrm{sig}_1(t) + \mathrm{sig}_2(t) + \eta(t), \end{cases} \quad (7)$$

where $\eta(t)$ is a Gaussian white noise signal, sig is the simulation signal with noise.

There are two parts in instantaneous frequency of (7), which could be described by mathematization as (8):

$$\begin{cases} f_1(t) = 800 + 80\ \cos\left(4\pi t\right), \\ f_2(t) = 350, \end{cases} \quad (8)$$

where t is the program running time, which values is [0, 1/fs, 1]. And fs is the sampling frequency in this simulation, and $fs = 1024$ Hz.

Before analysis the time-frequency of the simulation acoustic signal, the Gaussian white noise with signal-to-noise ratio of 10 dB was added which make the signal image more confusing, and closer to real situation, Doppler simulation is also carried out according to the method of reference [26]. The time-domain waveform with and without Gaussian white noise is shown in Figures 4 and 5, respectively.

3.2. Ridge Lines Extracting. The established simulation signal eliminated the Doppler distortion through the STFT, used by the method same as reference [14]. Figure 6 shows the time-frequency matrix after transform. As shown in Figure 6, the situation of time-frequency distribution reflects the change low between the instantaneous frequencies of the signal with time. According to (8), the instantaneous

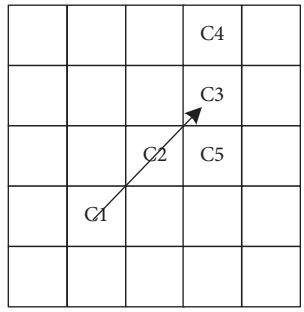

Figure 3: Schematic diagram of local optimal peak extraction.

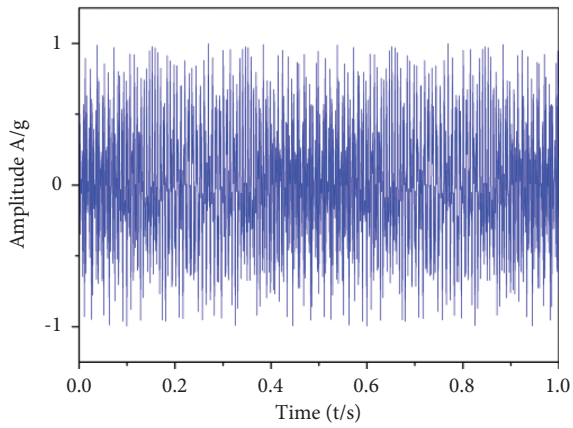

Figure 4: The time-domain waveform without noise of the analog signal.

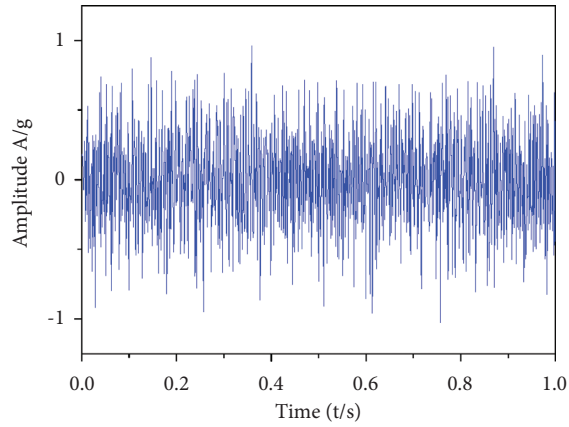

Figure 5: The time-domain waveform with 10 dB noise of the analog signal.

frequency of the analog signal should be a straight line and a sinusoid, and it could be found that the highlighted in Figure 6. And this proves the correctness of the simulation signal and the validity of the short-time Fourier transform.

The original algorithm and the improved algorithm are used to extract the time-frequency ridge of the established simulation signal, respectively. The number of movement(n) in both algorithms is 134. Figure 7 is the actual frequency

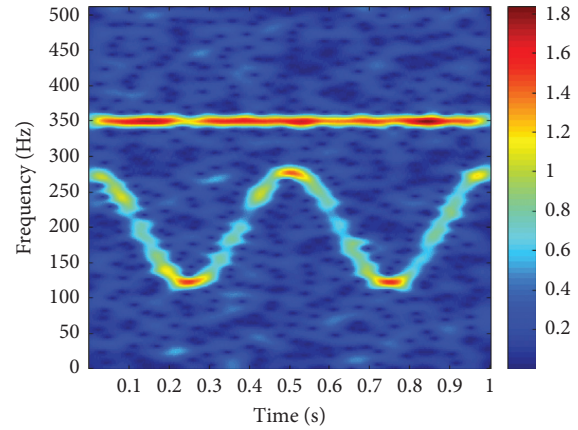

Figure 6: Short-time Fourier Transform of analog signal.

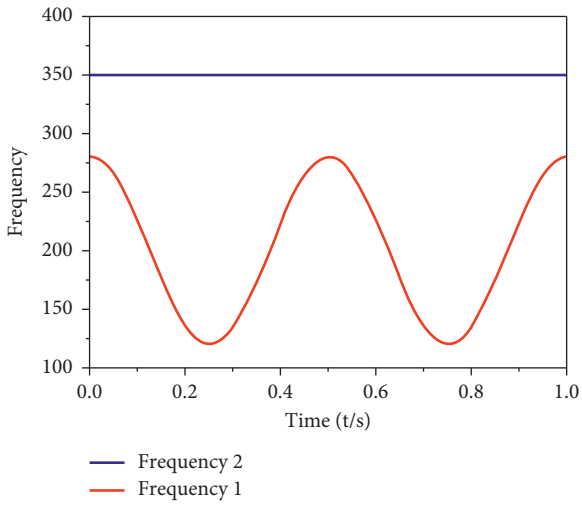

Figure 7: Actual frequency ridge lines.

ridge lines of the signal, and the Figure 8(a) and Figure 8(b) are the metric matrix and the ridge lines obtained by the improved Crazy Climber algorithm respectively. Figure 9(a) and Figure 9(b) are the metric matrix and the ridge lines obtained by the traditional algorithm. It can be found that the two ridge lines are significantly highlighted compared to other positions in Figure 8(a), but this situation is not obvious in Figure 9(a). Though the ridge line of frequency $f2$ has a higher metric value, the one of frequency $f1$ is not quite clear. And this may lead to an inability to extract the ridge line effectively. What's more, compare the measurement value in Figure 8(a) with the one in Figure 9(a), it can be found that the maximum measurement value on the ridge lines obtained by the improved Crazy Climber algorithm almost reached 700, but there is only 300 in Figure 9(a) which is obtained by the ordinary one. Meanwhile, by comparing Figures 8(b) and 9(b), it can be found that the traditional algorithm cannot extract the ridge line of $sig1(t)$, while the improved algorithm can clearly display the ridge lines of both signals. So that, the improved algorithm had better performance in extracting ridge lines compare with the ordinary one in the same number of movement.

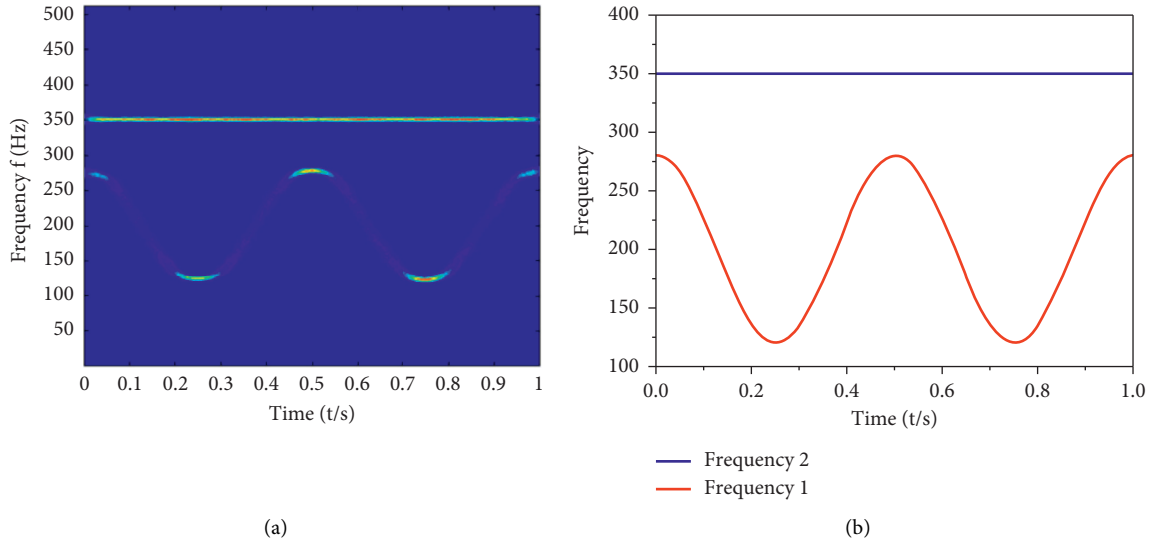

Figure 8: Metric matrix and the ridge lines obtained by the improved algorithm.

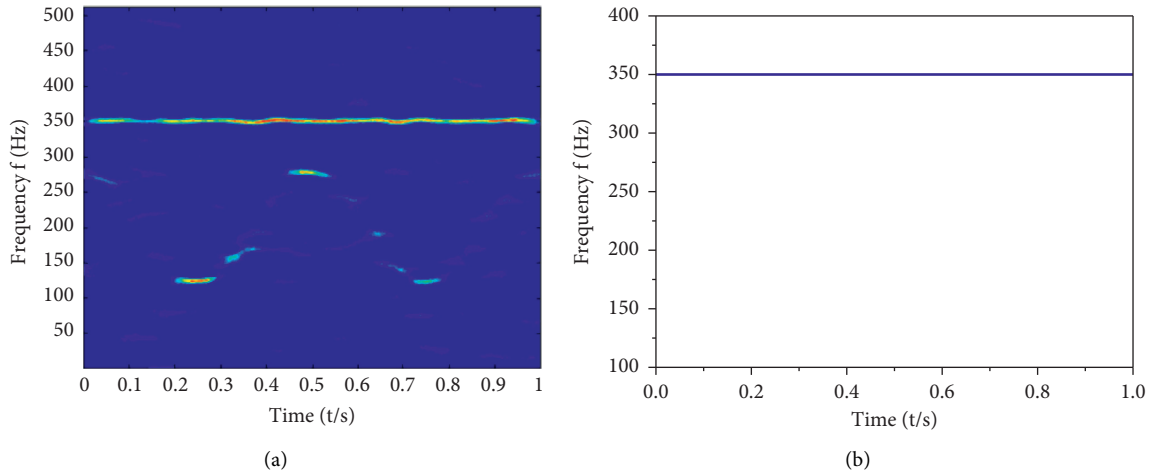

Figure 9: Metric matrix and the ridge lines obtained by the traditional algorithm.

The number of moves is continuously increased until the extraction accuracy of the traditional algorithm is close to that of the improved algorithm, and the number of moves of the traditional algorithm is close to 300. Compare the operating speed of two algorithms with the situation of same extraction accuracy. In order to minimize the influence of other factors as much as possible, ten tests were carried out for each algorithm, and the average results of ten tests were taken as the final result. The average operation time as shown in Table 1. It can be found that in Table 1, the average operation time of improved algorithm is about 0.87 s, while the traditional one will take more than 1.1 s Therefore, the amelioration of the algorithm can improve the operation speed to a certain degree.

In order to further verify the accuracy of the improved crazy climbing algorithm, the average deviation between the actual ridge line and the extracted ridge line was taken as the evaluation standard to evaluate the two algorithms. The calculation formula of this index is as follows:

$$\overline{\lambda} = \frac{\sum_{r=1}^{a} |Y_r - y_r|}{a}, \tag{9}$$

where a is the length of the extracted ridge line, Yr is the frequency value of the extracted ridge line at point r, and yr is the frequency value of the actual ridge line at point r.

The average deviation of two algorithms as shown in Table 2, and from the algorithm's accuracy, the average deviation is as small as possible. It can be found that the average deviation of the modified algorithm is close to zero and much smaller than it of the traditional algorithm, especially in the signal of the $sig2(t)$. So that it can prove the accuracy, operation speed and integrity of the improved Crazy Climber algorithm are better than that of the original algorithm.

Table 1: The average operation time of both algorithms.

Algorithm	$t1$ (s)	$t2$ (s)	$t3$ (s)	$t4$ (s)	$t5$ (s)	$t6$ (s)	$t7$ (s)	$t8$ (s)	$t9$ (s)	$t10$ (s)	t (s)
Improved	0.87	0.86	0.88	0.88	0.86	0.85	0.86	0.90	0.88	0.85	0.87
Ordinary	1.14	1.12	1.10	1.11	1.11	1.13	1.14	1.15	1.12	1.11	1.12

Table 2: The average deviation of two algorithm.

Algorithm	Average deviation for $sig1(t)$	Average deviation for $sig2(t)$
Improved	2.45 Hz	0
Ordinary	—	1.32

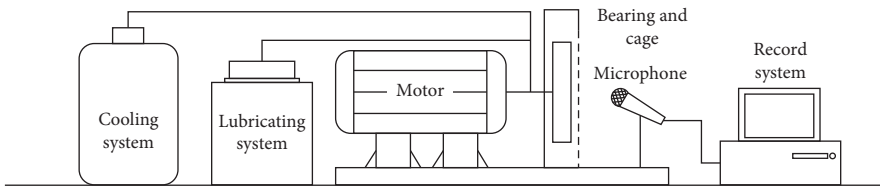

Figure 10: The schematic Figure of the experimental equipment.

4. Experimental Verification

The accuracy and efficiency of the algorithm are verified by simulation analysis, and the superiority of the proposed method is further verified by experiments. An experimental platform was designed to obtain the acoustic signals of train bearings in static states. In this experiment, the bearings of the railway locomotive were taken as the experiment subject. The outside diameter of the wheel is 840 mm and the diameter of the wheel bearing is 165 mm. There are 16 rollers in the bearing and the diameter is 25 mm. There is only one microphone in the experiment system which takes as signal acquisition equipment, the train speed in simulation is 25 m/s, therefore the spindle speed experiment is 1400 r/min.

The motor used in this experiment is Realland VFG, which the maximum revolving speed is 8000 rpm. The connection between the train bearing and the motor is rigid. The rotational movement of the bearing is driven by the motor, which could simulate the working state of the bearing when the train is running. In order to ensure the safety of the experiment, there is a protective device installed outside the bearing. And there is a cooling device and a lubricating device in the experiment system. Moreover, an operating data acquisition system is added to detect the running status of the experimental equipment. After the experiment started, the microphone began to collect the signal data when the bearing and motor ran smoothly. The schematic of the experimental equipment as shown in Figure 10.

Figure 11 represents the time domain waveform of the train bearing outer-ring in experiment, and the time-frequency matrix as shown in Figure 12. 4000 sample points were selected from the signal data which was collected by the microphone, and the STFT was used for time-frequency transformation to obtain the time-frequency matrix of the acoustic signal. The time-frequency spectrum of fault signal as shown in Figure 13. The improved and the ordinary Crazy Climber algorithm were used for extracting the ridge lines of the time-frequency matrix, respectively. Some key parameters were set as follows in the calculation process, the number of Climber movement is 200, the threshold value of the metric matrix is 0.1 times of the maximum measurement value, the length threshold value of the ridge lines is 0.5 times the width of the time-frequency matrix. The ridge lines obtained by improved and ordinary algorithms were shown in Figures 13(a) and 13(b), respectively.

As shown in the image, both algorithms could extract the ridge lines of the time-frequency matrix, but the ridge lines obtained by the ordinary Crazy Climber algorithm are not quite clear and exact relative to the improved one. On the other hand, the ridge lines extracted by the improved algorithm are more smooth and complete, and much closer to the ridge lines in reality. Therefore, the improved Crazy Climber algorithm is better than the original one overall.

According to (9), the average deviation between actual ridge line and extracted ridge line of the two algorithms under experimental conditions was calculated, as shown in Table 3. It can be seen from Table 3 that the average deviation of the improved algorithm is close to 0 Hz, while that of the traditional algorithm is around 1.5 Hz, which indicates that the ridge line obtained by the improved algorithm is closer to the real situation, and this also shows the accuracy of the improved algorithm to a certain extent. In order to further verify the deviation between the two algorithms, the number of movement of the traditional algorithm is constantly improved. When the accuracy of the traditional algorithm reaches that of the improved algorithm, the number of movement is 378. In the case of the same accuracy, the time consumption of the traditional algorithm is 1.12 s, and the time consumption of the improved algorithm is 0.83 s. Therefore, it can be judged that the improved algorithm is better than the traditional algorithm in accuracy and efficiency.

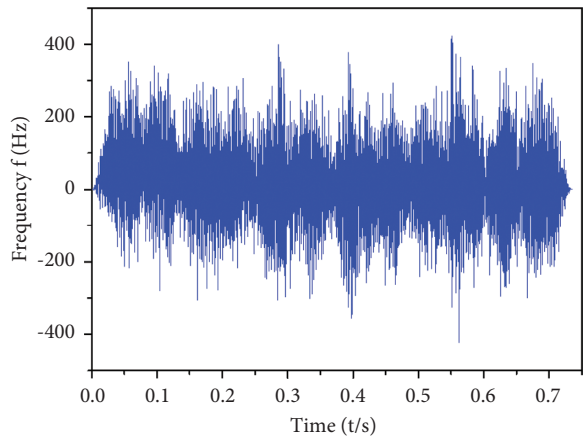

Figure 11: The time domain waveform of the train bearing.

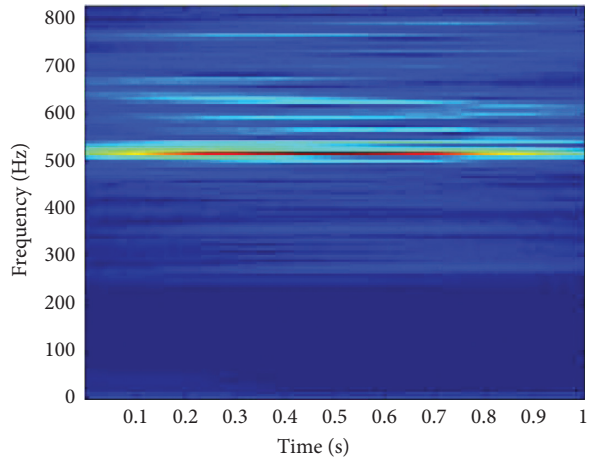

Figure 12: Time-frequency matrix of the train bearing.

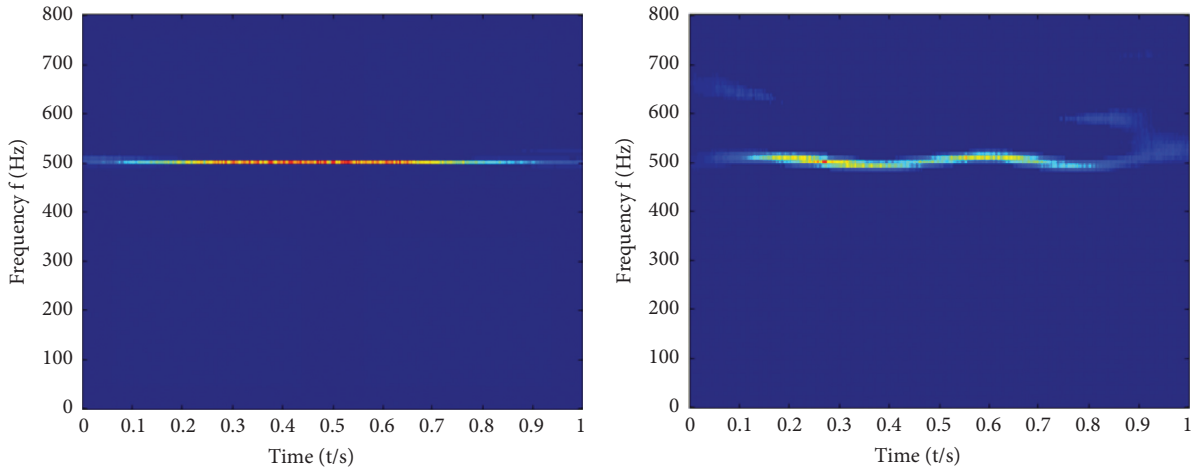

Figure 13: Time-frequency spectrum of fault signal adopted by two algorithms.

Table 3: The average deviation of two algorithm in experiment.

Algorithm	Average deviation for acoustic signal (Hz)
Improved	0.3
Ordinary	1.51

Furthermore, in order to verify whether the established algorithm can realize bearing fault diagnosis, the order of the ridge line proposed in Figure 12 is extracted. And the order of bearing outer ring fault is calculated according to (10).

$$O_o = 0.5z\left(1 - \frac{\mathrm{d}}{D}\cos\ \alpha\right), \tag{10}$$

where z is the number of the rollers. d is the diameter of the rolling body, D is the nodal diameter of the bearing, and the α is the contact angle.

According to the (10), the fault order of the outer ring can be obtained, which is 6.83. And the order of the ridge line also could be obtained by further calculation. However, there is no obvious fundamental ridge lines in the time-frequency diagram, so that, the extracted ridge line is not the corresponding fundamental frequency ridge line. What should be noticed is that, the fundamental frequency of the train bearing in this condition is 74.11 *Hz*. By calculating, it can be found that the average value of order is 6.787, which is close to the calculated order of the outer ring fault. And it can be judged that the outer ring is faulty, and the diagnosis result is consistent with the reality. The results show that the improved Crazy Climber algorithm proposed in this paper can realize the diagnosis of bearing faults in practical applications.

5. Conclusion

This paper proposes a novel denoise method based on the STFT and improved Crazy Climber algorithm. The time-frequency of the received acoustic signal was obtained by STFT. And for the Crazy Climber algorithm, the movement rule of Climber in the metric matrix and the fitting method of the ridge lines are improved. Then, the ridge lines in time-frequency domain are extracted accurately and efficiently. The effectiveness of the proposed method is verified by simulation and experiment on actual train bearing signals. The results show that the method proposed in this paper can effectively detect the train bearing, and the detection results are reliable and feasible. The features of this method are apparent as follows: (1) the movement law of the particle (climber) is improved, so that the particle can move to the high-energy area actively during the movement process, and can actively avoid the point already passed or low energy point, so that the particle can reach the high energy point more accurately and faster. (2) The ridge line fitting method in metric matrix is improved and the local optimal peak extraction method is proposed. In order to improve the speed, precision and smoothness of ridge line extraction, the center time of time-frequency curve is taken as the starting point and the point with higher height value is selected as the line point during the fitting process. (3) Through simulation and experiment, compared with the improved algorithm and the common algorithm, the proposed crazy climber algorithm has obvious advantages in calculation accuracy and efficiency, and can realize acoustic detection of train bearings.

It should be noted that the method proposed in this paper is mainly applied to noise reduction and detection of single bearing, and the effectiveness of the method is verified by theory and experiment. This provides some theoretical and technical support for The Wayside Acoustic Defective Bearing Detector System. However, according to the running process and detection results of the algorithm, it can be found that the algorithm can be applied to noise reduction and detection of multiple bearings. Therefore, in further work, the potential application of the proposed method in noise reduction and detection of two or more bearings will be involved and discussed.

Data Availability

The data of the acoustic signal used to support the findings of this study are included within the article.

Conflicts of Interest

The authors declare that there are no conflict of interest regarding the publication of this paper.

Acknowledgments

This work was supported by the National Science Foundation for Young Scientists of China (Grant no. 62001079).

References

[1] X. Chiementin, F. Bolaers, and J.-P. Dron, "Early detection of fatigue damage on rolling element bearings using adapted wavelet," *Journal of Vibration and Acoustics*, vol. 129, no. 4, pp. 495–506, 2007.

[2] Y. Lei, Z. He, and Y. Zi, "Application of a novel hybrid intelligent method to compound fault diagnosis of locomotive roller bearings," *Journal of vibration and acoustics-transactions of the Asme*, vol. 130, no. 3, pp. 569–583, 2008.

[3] R. Yan and R. X. Gao, "Rotary machine health diagnosis based on empirical mode decomposition," *Journal of Vibration and Acoustics*, vol. 130, no. 2, pp. 53–64, 2008.

[4] J. Dybala and R. Zimroz, "Rolling bearing diagnosing method based on Empirical Mode Decomposition of machine vibration signal," *Applied Acoustics*, vol. 77, pp. 195–203, 2014.

[5] H. C. Choe, Y. Wan, and A. K. Chan, "Neural Pattern Identification of railroad Wheel-Bearing Faults from Audible Acoustic Signals: Comparison of FFT, CWT, and DWT Features," in *Proceedings of the SPIE Proceedings on Wavelet Applications*, Orlando, FL, USA, April 1997.

[6] Y. Yuan, X. Zhao, J. Fei, Y. Zhao, and J. Wang, "Study on fault diagnosis of rolling bearing based on time-frequency generalized dimension," *Shock and Vibration*, vol. 2015, Article ID 808457, 11 pages, 2015.

[7] Z. Ma, W. Ruan, M. Chen, and X. Li, "An improved time-frequency analysis method for instantaneous frequency estimation of rolling bearing," *Shock and Vibration*, vol. 2018, Article ID 8710190, 18 pages, 2018.

[8] M. Zhang, X. Huang, Y. Li, H. Sun, J. Zhang, and B. Huang, "Improved continuous wavelet transform for modal parameter identification of long-span bridges," *Shock and Vibration*, vol. 2020, Article ID 4360184, 16 pages, 2020.

[9] J. E. Cline, J. R. Bilodeau, and R. L. Smith, "Acoustic Wayside Identification of Freight Car Roller Bearing Defects," in *Proceedings of the 1998 ASME/IEEE joint railroad conference*, IEEE, Philadelphia, PA, USA, April 1998.

[10] D. Barke and W. K. Chiu, "Structural health monitoring in the railway industry: a review," *Structural Health Monitoring*, vol. 4, no. 1, pp. 81–93, 2005.

[11] I. Firdausid and C. Wu, "Development and deployment of advanced wayside condition monitoring system," *Foreign Rolling Stock*, vol. 39, no. 2, pp. 39–45, 2002.

[12] L. Yu-xing and W. Long, "A novel noise reduction technique for underwater acoustic signals based on complete ensemble empirical mode decomposition with adaptive noise, minimum mean square variance criterion and least mean square adaptive filter," *Defence Technology*, vol. 16, no. 3, pp. 543–554, 2020.

[13] Q. Ni, J. C. Ji, K. Feng, and B. Halkon, "A fault information-guided variational mode decomposition (FIVMD) method for rolling element bearings diagnosis," *Mechanical Systems and Signal Processing*, vol. 164, Article ID 108216, 2022.

[14] A. Zhang, F. Hu, Q. He, C. Shen, F. Liu, and F. Kong, "Doppler shift removal based on instantaneous frequency estimation for wayside fault diagnosis of train bearings," *Journal of Vibration and Acoustics, Transactions of the Asme*, vol. 136, no. 2, 2014.

[15] X. Xu, W. Wang, J. Liu, and S. Sun, "Instantaneous frequency components separation method based on synchro-squeezed short time Fourier transform," *Journal of Vibration Engineering*, vol. 31, no. 6, pp. 1085–1092, 2018.

[16] R. A. Carmona, W. L. Hwang, and B. Torresani, "Multiridge detection and time-frequency reconstruction," *IEEE Transactions on Signal Processing*, vol. 47, no. 2, pp. 480–492, 1999.

[17] K Kailiang Xu, D Dean Ta, and W Weiqi Wang, "Multiridge-based analysis for separating individual modes from multimodal guided wave signals in long bones," *IEEE Transactions on Ultrasonics, Ferroelectrics, and Frequency Control*, vol. 57, no. 11, pp. 2480–2490, 2010.

[18] H. Li, J. D. Wen, J. Zhang, and B. C. Wen, "Research on characteristics of chaotic motion based on the wavelet ridge," *Advanced Engineering Forum*, vol. 2, pp. 765–768, 2011.

[19] X. Chen and K. Xu, "Wavelet ridge Analysis of Lamb Wav," *In Advanced Materials Research*, vol. 457, pp. 484–487, 2012.

[20] C. Dou and J. Lin, "Ridge extraction based on adaptive variable-bandwidth cost functions by edge detection of time frequency images," *Measurement Science and Technology*, vol. 31, no. 5, Article ID 55402, 2020.

[21] K. Dziedziech, W. J. Staszewski, A. Ghosh, B. Basu, and T. Uhl, "Characterisation of instantaneous dynamic parameters in vibration analysis of tuned liquid column dampers," *Nonlinear Dynamics*, vol. 90, no. 1, pp. 717–731, 2017.

[22] K. Ren, L. Du, X. Lu, Z. Zhuo, and L. Li, "Instantaneous frequency estimation based on modified kalman filter for cone-shaped target," *Remote Sensing*, vol. 12, no. 17, p. 2766, 2020.

[23] L. Meng, X. Xu, and Y. Zuo, "Fault feature extraction of logarithmic time-frequency ridge order spectrum of planetary gearbox under time-varying conditions," *Journal of Vibration and Shock*, vol. 39, no. 7, pp. 163–169, 2020.

[24] Y. Zheng, R. Fan, C. Qiu, Z. Liu, and D. Tian, "An improved algorithm for peak detection in mass spectra based on continuous wavelet transform," *International Journal of Mass Spectrometry*, vol. 409, pp. 53–58, 2016.

[25] F. Hu, C. Q. Shen, and F. R. Kong, "De-noising Method for Wayside Train Bearings Acoustic Signal Based on Doppler Shift," *Applied Mechanics and Materials*, vol. 333, pp. 504–509, 2013.

[26] C. Wang, F. Hu, Q. He, A. Zhang, F. Liu, and F. Kong, "De-noising of wayside acoustic signal from train bearings based on variable digital filtering," *Applied Acoustics*, vol. 83, pp. 127–140, 2014.

[27] Y. Lin and Y. Zhang, "Improved crazy climber algorithm and its application in obtaining frequency-hopping pattern," *Application Research of Computers*, vol. 31, no. 6, pp. 1684–1687, 2014.

[28] Y. Peng, X. Guo, Y. Xing et al., "A Method for Velocity Signal Reconstruction of AFDISAR/PDV Based on Crazy-Climber Algorithm," in *Proceedings of the AOPC 2017 Fiber Optic Sensing and Optical Communications*, SPIE, Beijing, China, October 2017.